Journal of Alloys and Compounds 509 (2011) 165–171

Contents lists available at ScienceDirect

Journal of Alloys and Compounds

journal homepage: www.elsevier.com/locate/jallcom

Stability and electronic structure of the Co–P compounds from first-principle calculations

Zhenhua Yang[a,b,c], Li Liu[a,b,c], Xianyou Wang[a,b,c,*], Shunyi Yang[c], Xuping Su[c]

[a] School of Chemistry, Key Laboratory of Environmentally Friendly Chemistry and Applications of Ministry of Education, Xiangtan University, Xiangtan 411105, Hunan, China
[b] Faculty of Materials, Optoelectronics and Physics, Key Laboratory of Low Dimensional Materials & Application Technology of Ministry of Education, Xiangtan University, Xiangtan 411105, Hunan, China
[c] Key Laboratory of Materials Design and Preparation Technology of Hunan Province, Xiangtan University, Xiangtan 411105, Hunan, China

ARTICLE INFO

Article history:
Received 19 April 2010
Received in revised form 31 August 2010
Accepted 1 September 2010
Available online 21 September 2010

Keywords:
First-principle
Co–P compounds
Stability
Electronic properties
Covalent and ionic components

ABSTRACT

First-principle calculations based on density functional theory (DFT) were performed to investigate the structural stability and electronic properties of Co–P compounds such as Co_2P(I) (orthorhombic), Co_2P(II) (hexagonal), CoP, CoP_2 and CoP_3. The cohesive energies of Co–P compounds are all negative, which indicates that they are thermodynamically stable. Furthermore, the stability of Co–P compounds decreases with the increase of P element. By analyzing the electronic structures of Co–P compounds, we have found that Co_2P(I) (orthorhombic), Co_2P(II) (hexagonal) and CoP show metallic character, while CoP_2 and CoP_3 show semiconductor character. The bonding behaviour between Co atom and P atom in Co–P compounds is a combination of covalent and ionic nature.

1. Introduction

Lithium ion batteries have been widely used in the world and gradually become the leading power source in the 21st century due to their advantages, such as high theoretic capacity, high voltage, a low self-discharge rate and good cycling stability [1,2]. Carbon materials are commercially used as the anode material for lithium ion batteries. However, the theoretical capacity of carbon materials is only 372 mAh/g [3,4]. In order to get higher capacities, great efforts have been dedicated to investigate anode materials with larger energy density than graphite in recent years [5–8].

P-based compounds used as anode materials for lithium ion battery have attracted great interest because of their large initial gravimetric capacity [9–15]. For example, it has been reported that CoP electrode shows initial capacity of around 510 mAh/g and its capacity remains at around 400 mAh/g after 8 cycles, while mixture (CoP_3 + CoP) electrode exhibits initial capacity of around 880 mAh/g and its capacity remains at about 400 mAh/g after 8 cycles [14]. By comparison, CoP electrode has better cyclic stability than CoP_3 electrode. Moreover, it is reported that CoP has better electronic conductivity than CoP_3 through experiments [14].

Due to excellent properties of Co–P compounds, the synthesis technologies have been extensively investigated [16–18] and the structural analysis has also been conducted in order to understand the intrinsic mechanism [19–23]. By the linear muffin-tin orbital method in the atomic sphere approximation (LMTO-ASA), it has been found that Co_2P with hexagonal structure exhibits ferromagnetism while Co_2P with orthorhombic structure reveals non-magnetic character [19]. Strong Co–P and weak P–P bonding interactions in CoP were confirmed by X-ray photoelectron spectroscopy [20]. The electronic structure of CoP_3 has been investigated by X-ray photoelectron spectroscopy, and it has been found that a plasmon loss satellite peak occurs in the Co 2p spectra of CoP_3 [21]. Besides, the electronic structure of CoP_3 has also been studied using first-principle calculations at the GGA level [22,23].

Although the electronic structures of Co_2P and CoP_3 have been studied, the investigations for the electronic structures of CoP and CoP_2 have not been found. And the structural stability of Co–P compounds has not been reported. Hence, it is necessary to study the relationships between crystal structure, structural stability and electronic structure of Co–P compounds in detail.

Because Co_3P only exists in solid solutions but it is nonexistent under usual conditions [24], Co_3P compound is not taken into consideration. In this paper, first-principle calculations based on density functional theory were implemented to investigate the crystal structure, structural stability and the bonding mechanism

* Corresponding author: Tel.: +86 731 58292060; fax: +86 731 58292061.
E-mail address: wxianyou@yahoo.com (X. Wang).

0925-8388/$ – see front matter © 2010 Elsevier B.V. All rights reserved.
doi:10.1016/j.jallcom.2010.09.018

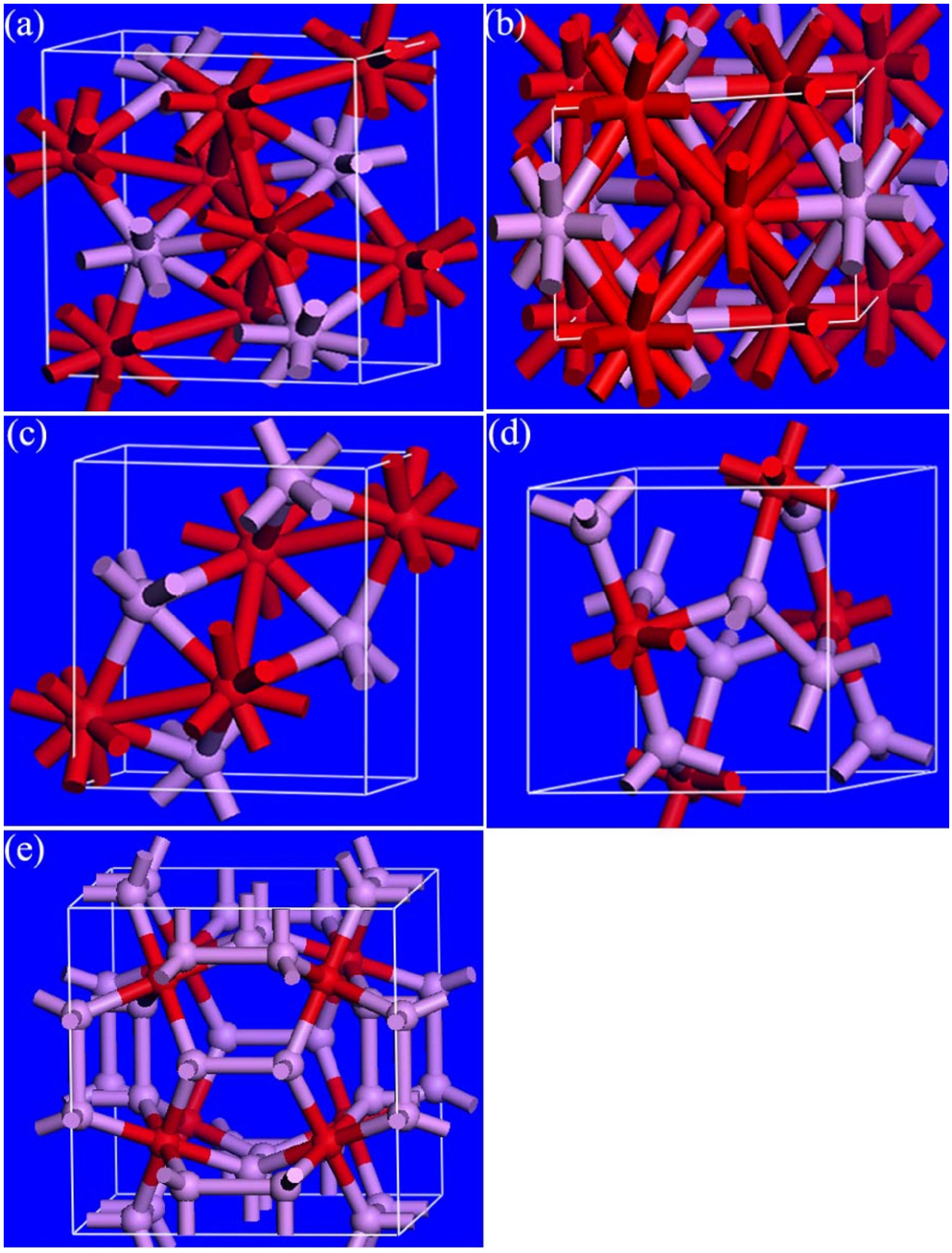

Fig. 1. The crystal structure of Co–P compounds illustrated by ball and stick model. Co_2P(I) (a), Co_2P(II) (b), CoP (c), CoP_2 (d) and CoP_3 (e). Dark-colored (red) circle refers to cobalt atom and light-colored (purple) circle refers to phosphorus atom. (For interpretation of the references to colour in this figure legend, the reader is referred to the web version of the article.)

of Co_2P(I) (orthorhombic), Co_2P(II) (hexagonal), CoP, CoP_2 and CoP_3 compounds.

2. Computational method

The calculations have been performed using the ab inito total-energy and molecular-dynamics program VASP (Vienna ab initio simulation program) developed at the institut für Materialphysik of the Universität Wien [25–28]. The exchange and correlation energies for GGA (generalized gradient approximation) were treated, using the PBE scheme and the Projector Augmented Wave (PAW) pseudopotentials. The convergence of the calculations is related to both energy cut-off and *k*-points grid. To ensure a good convergence for total energy and forces acting on the atoms, the energy cutoff was set to 350 eV and Monkhorst-Pack grid ($10 \times 10 \times 10$) was used for k point sampling in the first irreducible Brillouin zone. For the calculation of the electronic density of states, the tetrahedron method with Bloch corrections was used with $13 \times 13 \times 13$ grid. For each Co–P composition, the model of Co–P binary compounds were relaxed, using a Quasi Newton (QN) algorithm to optimize both atomic positions and lattice constants with symmetry constraints until the forces on the atoms converged to less than 0.01 eV/Å. Spin polarized calculations were considered to check the occurrence of Co–Co magnetic interaction.

Cohesive energy is often defined as the work which is needed when crystal decomposes into the single atom. Therefore, it is an important physical quantity to describe the strength of bonds, by which we can assess the stability of Co–P binary compounds. In this paper, in order to obtain cohesive energy value correctly, the total energy for the crystal and the free atoms were calculated based on a cubic supercell (fcc-box) that contains the corresponding atoms. The fcc-box has the lattice constant of 15 Å. The cohesive energy E_c of Co_xP_y can be expressed as follows [29–31]:

$$E_c = \frac{1}{x+y}(E_{tot}^{Co_xP_y} - xE_{atom}^{Co} - yE_{atom}^{P})$$

Table 1
Crystallographic data of Co–P compounds.

Compound	Crystal system	Pearson symbol	Atom numbers	Space group
Co_2P(I) [32]	Orthorhombic	oP12	12	Pnma
Co_2P(II) [33]	Hexagonal	hP9	9	P-62m
CoP [34]	Orthorhombic	oP12	8	Pnma
CoP_2 [35]	Monoclinic	mP12	12	P121/c1
CoP_3 [36]	Cubic	cI32	16	Im-3

Table 2
Lattice parameters of experimental structures and calculated structures of Co–P compounds.

Compound	Lattice parameters (Å)	
	Experiment	Calculated result (first principle calculations)
Co_2P(I)	a = 5.649 [32] b = 3.513 [32] c = 6.607 [32]	a = 5.519 b = 3.507 c = 6.587
Co_2P(II)	$a = b$ = 5.742 [33] c = 3.457 [33]	$a = b$ = 5.723 c = 3.406
CoP	a = 5.077 [34] b = 3.281 [34] c = 5.587 [34]	a = 5.063 b = 3.270 c = 5.554
CoP_2	a = 5.551 [35] b = 5.549 [35] c = 5.614 [35]	a = 5.543 b = 5.547 c = 5.615
CoP_3	$a = b = c$ = 7.711 [36]	$a = b = c$ = 7.716

where $E_{tot}^{Co_xP_y}$ is the electronic total energy of primitive cell of Co_xP_y; E_{atom}^{Co} and E_{atom}^{P} are the electronic total energies of the isolated Co atom and P atom in freedom states, respectively.

In order to validate the computational method, the equilibrium lattice parameters of Co_2P(I), Co_2P(II), CoP, CoP_2, and CoP_3 have been computed as compared with the experimental results.

3. Results and discussion

3.1. Structural model and lattice parameters

Ball-and-stick models of the crystal structures of Co_2P(I), Co_2P(II), CoP, CoP_2 and CoP_3 are illustrated in Fig. 1. Available experimental data on the crystallographic data of this alloy system are summarized in Table 1. The lattice parameters are given in Table 2, together with the available experimental data. Table 2 reveals that calculated lattice parameters are in fairly good agreement with the experimental results due to the errors within ±1% except for Co_2P(I) within ±3%.

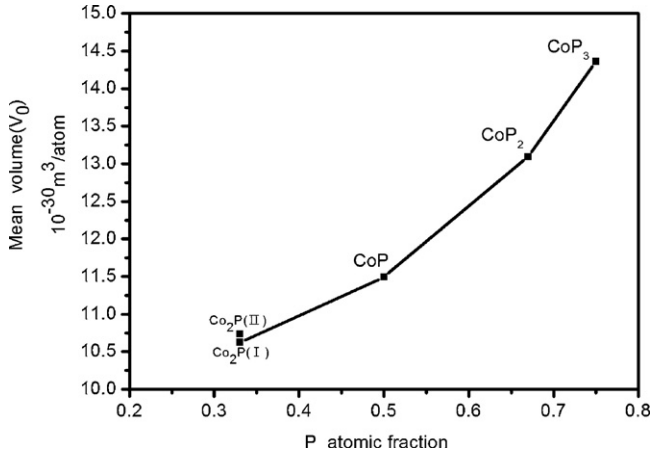

Fig. 2. The mean volume per atom for the Co–P compounds.

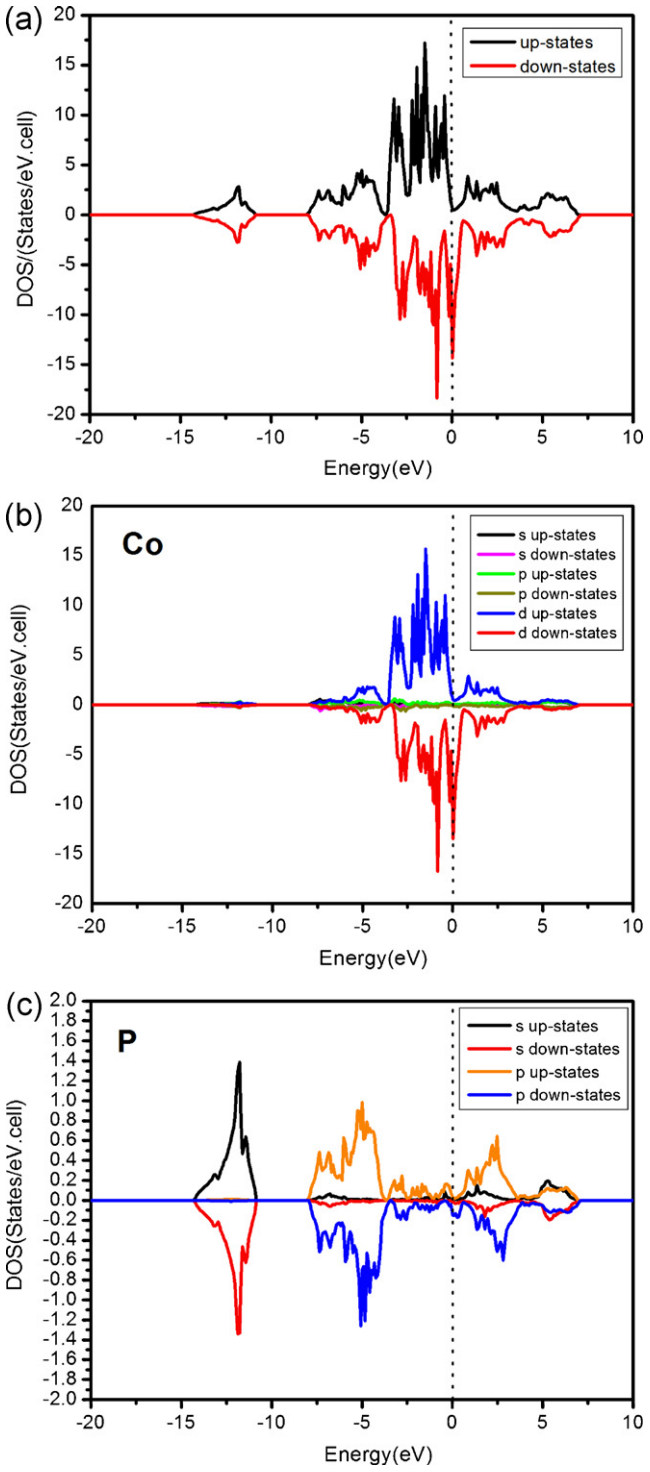

Fig. 3. Calculated spin-polarized total density of states for Co_2P(II) (a); calculated partial density of states for Co_2P(II): Co atoms (b); P atoms (c).

3.2. Phase stability and cohesive properties of Co–P compounds

After the calculation of cohesive energy for Co–P compounds, it was found that the cohesive energy per atom for Co_2P(I), Co_2P(II), CoP, CoP_2 and CoP_3 are −5.64, −5.60, −5.30, −4.85 and −4.62 eV, respectively. The cohesive energies of Co_2P(I),

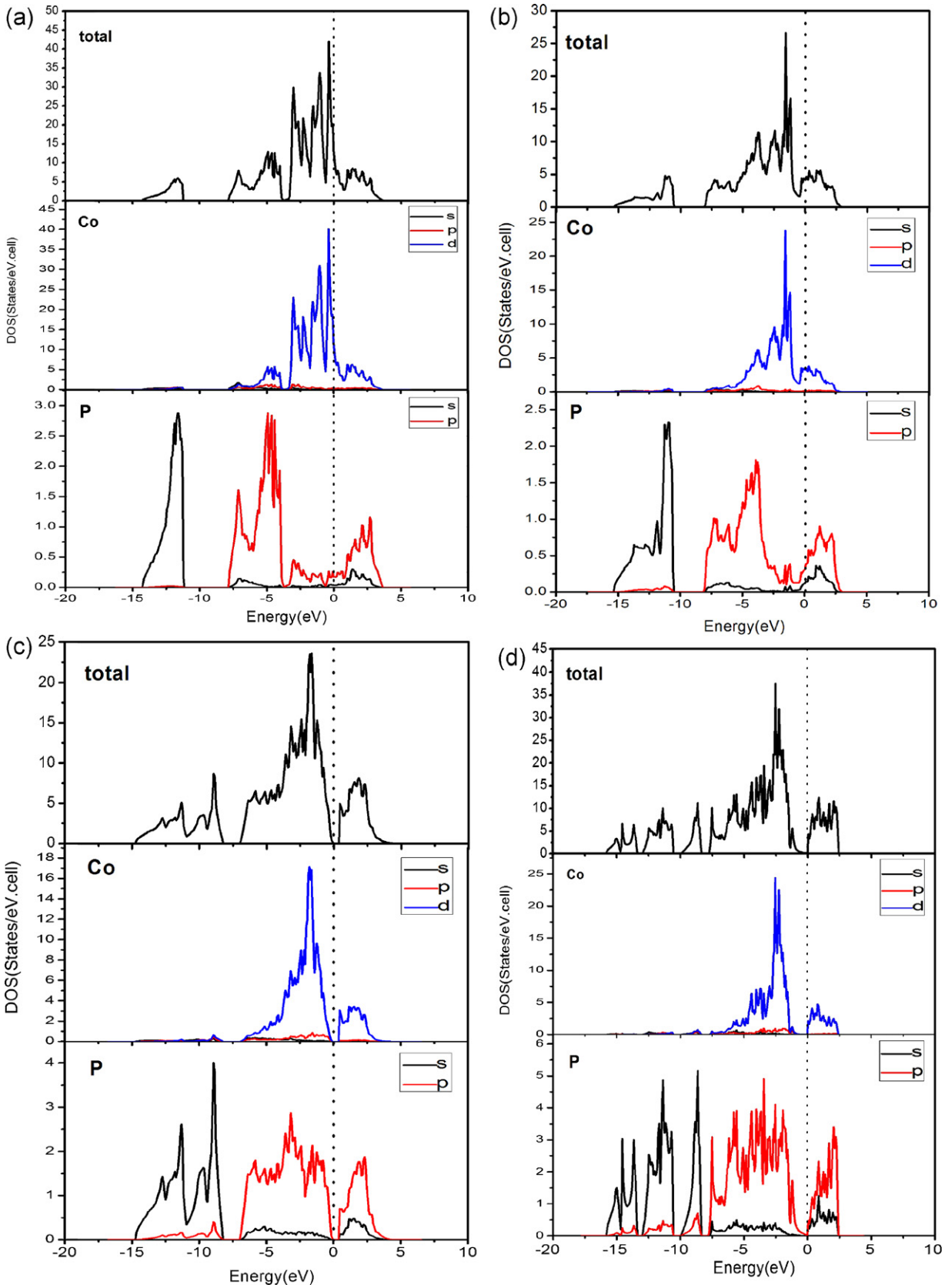

Fig. 4. Calculated total and partial density of states (DOS) for Co_2P(I) (a), CoP (b), CoP_2 (c) and CoP_3 (d). Vertical dotted lines indicate the Fermi energy level.

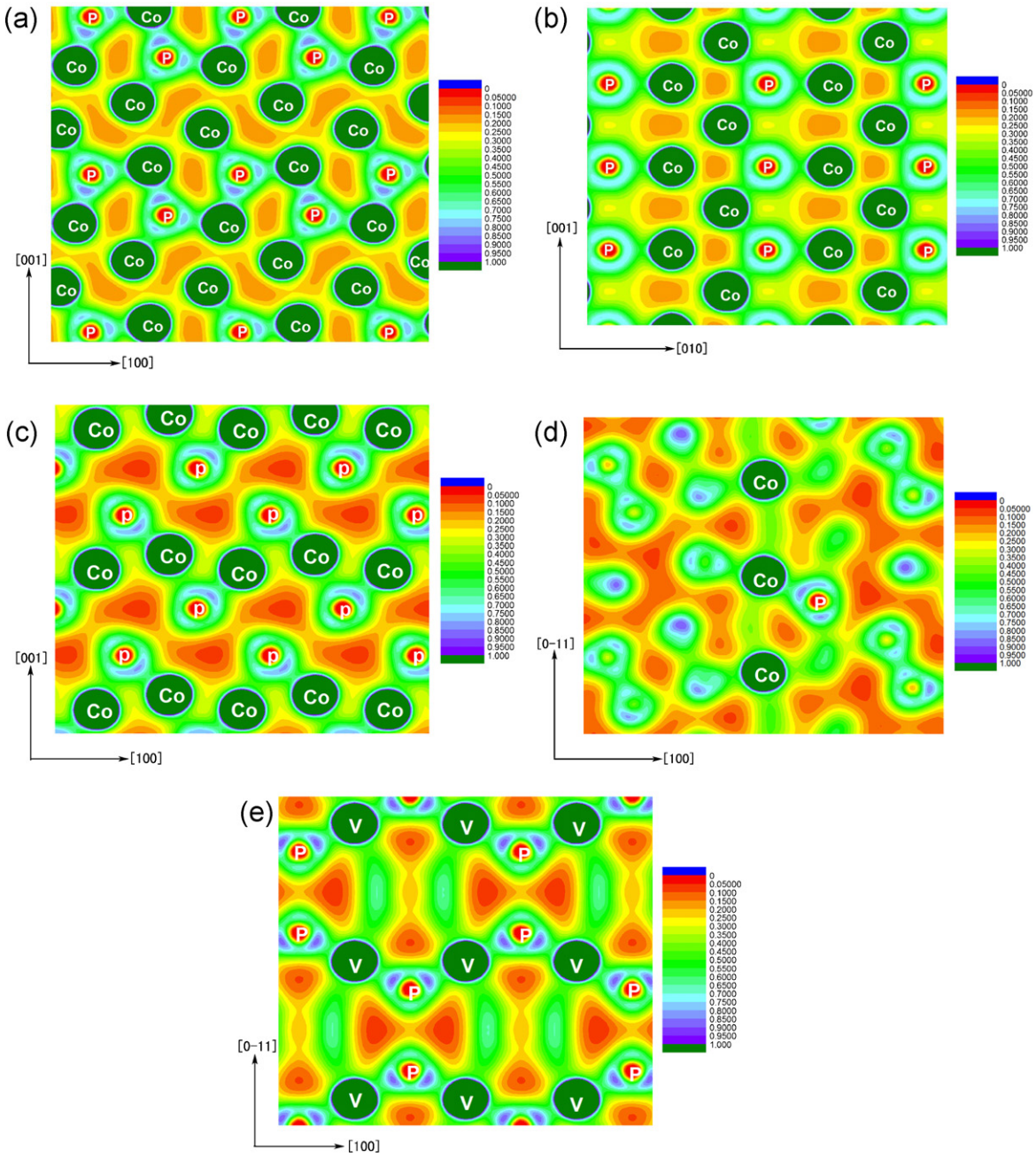

Fig. 5. Distribution maps of total charge densities in the (0 1 0) plane of Co_2P(I) (a) and CoP (c), (1 0 0) plane of Co_2P(II) (b), (0 1 1) plane of CoP_2 (d) and CoP_3 (e). These represent sections of the charge densities and charge density is in an increment of 0.05 e/Å^3 from 0 to 1.0 e/Å^3.

Co_2P(II), CoP, CoP_2 and CoP_3 are all negative, which indicate that these compounds are stable. A shift towards higher cohesive energy has been found with the increase of P element content. Hence, Co_2P has better stability with the orthorhombic structure than with the hexagonal structure and the stability of Co–P compounds decreases with the increase of P element content.

Additionally, the mean volume per atom for Co–P compounds was shown in Fig. 2. As can be seen from Fig. 2, the mean volume per atom increased with the increase of P content, which indicates good relationship between the mean volume per atom and cohesive energy. If the cohesive energy is more negative, the strength of bonds between Co and P will become stronger. As a result, the volume will become smaller with the shortening of the bond.

3.3. *Electronic structural properties and bonding mechanism in Co–P compounds*

To understand further electronic structure and structural stability, the density of states (DOS) of Co_2P(I), Co_2P(II), CoP, CoP_2 and CoP_3 with different types of structure was calculated and analyzed. Fig. 3(a) shows the total density of states (TDOS) of Co_2P(II) while Fig. 3(b) and (c) shows the partial density of states (PDOS) of Co_2P(II). The Fermi level is set to be at 0 eV in Fig. 3. The lowest valence band ranging from −14.5 to −10.5 eV is mostly composed of P 3s character. The upper valence band ranges from −8.0 eV to Fermi level and constitutes the hybridization of Co 3d and P 3P character. No band gap near Fermi level can be seen, indicating the metallic nature of CoP_2(II). Besides this, it can be concluded from TDOS that Co_2P(II) displays mag-

netic character. This is consistent with the result of previous literature [19].

Total and partial density of states of Co_2P(I), CoP, CoP_2 and CoP_3 are shown in Fig. 4(a)–(d), respectively. The Fermi level is set to be at 0 eV in Fig. 4. The TDOS of Co–P compounds were divided into three energy regions according to the PDOS: (1) Region 1, the lowest energy region mostly originating from P 3s character; (2) Region 2, the upper region of the valence band mostly originating from the mixture of Co 3d character and P 3p character; and (3) Region 3, the energy region just above Fermi level dominated by unoccupied Co 3d and P 3p character. From these plots, it can be seen that Co_2P(I) and CoP compounds show metallic character while CoP_2 and CoP_3 compound show semiconductor character according to the TDOS at the Fermi level. Furthermore, it is clear that the TDOS of Co–P compounds decreases with the increase of P content and the TDOS at the Fermi level for Co_2P(I) is the largest one, suggesting that the increase of P content could impair electronic conductivity. Besides, it was found that Co 3d character and P 3p character for Co_2P(I) and CoP show weak p–d hybridization, while Co 3d character and P 3p character for CoP_2 and CoP_3 show strong p–d hybridization between −8 eV and Fermi level.

In order to further explain electronic structure, the bonding electron number per atom was analyzed in the energy areas between −8 eV and Fermi level for Co_2P(I), Co_2P(II), CoP, CoP_2 and CoP_3. The results indicate that the bonding electron number per atom is 7.07 for Co_2P(I), 6.91 for Co_2P(II), 5.97 for CoP, 4.97 for CoP_2 and 4.44 for CoP_3, respectively. It is evident from these results that the bonding number per atom shifts to lower level with the increase of P content in crystal. Bonding electrons mainly come from the electrons located at the area between −8 eV and Fermi level. Therefore, the more bonding electrons there are, the stronger the charge interactions will be. Hence, Co_2P has better stability with the orthorhombic structure than with the hexagonal structure and the stability of Co–P compounds will gradually become worse with the increase of P content and CoP_3 compound has the worst structural stability. The result is well consistent with the variation of cohesive energy for Co–P compounds mentioned above.

To further explore the bonding nature in Co–P compounds structure, the charge density distribution of Co_xP_y is studied. Fig. 5(a)–(e) illustrates the total charge density map in the (0 1 0) plane for Co_2P(I), (1 0 0) plane for Co_2P(II), (0 1 0) plane for CoP, (0 1 1) plane for CoP_2 and (0 1 1) plane for CoP_3, respectively. It is obviously shown that weak covalent bonding exists between the P atoms, which results from the s–p interactions as shown in Fig. 5. Meanwhile, it can be seen from Fig. 5 that the charge density around P atoms exhibits a strong directional distribution toward Co atoms and the remarkable charge distribution overlap between Co atom and P atoms in all cases, clearly indicating the feature of covalent bond between Co atom and P atom.

In order to analyze the bonding mechanism quantitatively, the Bader analysis based on the AIM theory [37–39] was used to describe charge transfer quantitatively. In this approach, each atom of a crystal is surrounded by an effective surface that runs through minima of the charge density, and the total charge of an atom (so-called Bader charge, Q^B) is determined by the integration within this region [40]. The differences (ΔQ) between calculated atomic Q^B and charges derived from a purely ionic model for Co–P compounds are listed in Table 3. The negative values indicate that the atom loses electrons while the positive values indicate that the atom obtains electrons during the bonding process. The results show that charge transfers from Co basins to P basins. It is found that each P atom obtains 0.60 electrons from Co atoms for Co_2P(I) and 0.65 electrons from Co atoms for Co_2P(II), 0.35 electrons transfer from each Co atom to P atom for CoP, 0.32 electrons transfer from each Co atom to P atom for CoP_2 and 0.30 electrons transfer from each Co atom to P atoms for CoP_2. It is obvious that Co–P bond show ionic character in these Co–P compounds. On the basis of PDOS and charge density analysis, it can be concluded that the Co–P bond is a mixture of covalent and ionic contributions.

Table 3
Atomic charges (in e) for Co and P as obtained from a purely ionic model (Q^i), Bader analysis (Q^B) and their differences ($\Delta Q = Q^B - Q^i$).

Compound	Atoms	Bader electrons (Q^B)	Q^i	$\Delta Q = Q^B - Q^i$
Co_2P(I)	Co(1)	8.78	9	−0.22
	Co(2)	8.62	9	−0.38
	P	5.60	5	0.60
Co_2P(II)	Co(1)	8.75	9	−0.25
	Co(2)	8.60	9	−0.40
	P	5.65	5	0.65
CoP	Co	8.65	9	−0.35
	P	5.35	5	0.35
CoP_2	Co	8.68	9	−0.32
	P(1)	5.18	5	0.18
	P(2)	5.14	5	0.14
CoP_3	Co	8.70	9	−0.30
	P(1)	5.08	5	0.08
	P(2)	5.13	5	0.08
	P(3)	5.10	5	0.14

4. Conclusions

First-principle calculations based on the DFT have been used to study the structural stability and electronic properties of Co_2P(I), Co_2P(II), CoP, CoP_2 and CoP_3. The calculated equilibrium lattice constant is in good agreement with the experimental value.

The calculated results show that Co_2P has better stability with the orthorhombic structure than with the hexagonal structure and the stability of Co–P compounds will decrease with the increase of P element content, and CoP_3 has the worst structural stability. Co_2P(I), Co_2P(II) and CoP show metallic character while CoP_2 and CoP_3 show semiconductor character. And the increase of P content could impair the electronic conductivity of Co–P compounds. Besides, it can be concluded that the bond between Co atom and P atom is a mixture of covalent and ionic components.

Acknowledgements

This work is financially supported by National Natural Science Foundation of China (Grant No. 20871101), Scientific Research Fund of Hunan Provincial Education Department (Grant No. 09C945) and Scientific Research Fund of Xiangtan University (Grant No. 09XZX10).

References

[1] T. Yuan, R. Cai, R. Ran, Y.K. Zhou, Z.P. Shao, J. Alloys Compd. 505 (2010) 367.
[2] Y. Liang, Z.G. Tian, H.J. Liu, R. Peng, J. Alloys Compd. 504 (2010) 50.
[3] H.L. Zhao, Z.M. Zhu, C.L. Yin, H. Guo, D.H.L. Ng, Mater. Chem. Phys. 110 (2008) 201.
[4] H. Liu, D. Wexler, G.X. Wang, J. Alloys Compd. 487 (2009) L24.
[5] M.V. Koudriachova, Chem. Phys. Lett. 458 (2008) 108–112.
[6] V.L. Chevrier, J.W. Zwanziger, J.R. Dahn, J. Alloys Compd. 496 (2010) 25–36.
[7] D.W. Zhang, S.Q. Zhang, Y. Jin, T.H. Yi, S. Xie, C.H. Chen, J. Alloys Compd. 415 (2006) 229–233.
[8] L. Lacroix-Orio, M. Tillard, C. Belin, Solid State Sci. 10 (2008) 5–11.
[9] S.L. Liu, Y.T. Qian, L.Q. Xu, Solid State Commun. 149 (2009) 438–440.
[10] X.J. Wang, F.Q. Wan, J. Liu, Y.J. Gao, K. Jiang, J. Alloys Compd. 474 (2009) 233–236.
[11] Y.H. Cui, M.Z. Xue, X.L. Wang, K. Hu, Z.W. Fu, Electrochem. Commun. 11 (2009) 1045–1047.
[12] V. Pralong, D.C.S. Souza, K.T. Leung, L.F. Nazar, Electrochem. Commun. 4 (2002) 516–520.
[13] R. Alcántara, J.L. Tirado, J.C. Jumas, L. Monconduit, J. Olivier-Fourcade, J. Power Sources 109 (2002) 308–312.

[14] Z.S. Zhang, J. Yang, Y.N. Nuli, B.F. Wang, J.Q. Xu, Solid State Ionics 176 (2005) 693–697.
[15] M.G. Kim, J. Cho, Adv. Funct. Mater. 19 (2009) 1497–1514.
[16] S.L. Liu, Y.T. Qian, X.C. Ma, Mater. Lett. 62 (2008) 11–14.
[17] B.M. Barry, E.G. Gillan, Chem. Mater. 21 (2009) 4454–4461.
[18] E. Bekaert, J. Bernardi, S. Boyanov, L. Monconduit, M.-L. Doublet, J. Phys. Chem. C 112 (2008) 20481–20490.
[19] S. Fujii, S. Ishida, S. Asano, J. Phys. F: Met. Phys. 18 (1988) 971–980.
[20] A.P. Grosvenor, S.D. Wik, R.G. Cavell, A. Mar, Inorg. Chem. 44 (2005) 8988–8998.
[21] A.P. Grosvenor, R.G. Cavell, A. Mar, Phys. Rev. B 74 (2006) 125102.
[22] K. Mangersnes, O.M. Løvvik, Ø. Prytz, New J. Phys. 10 (2008) 053004.
[23] Ø. Prytz, O.M. Løvvik, J. Taftø, Phys. Rev. B 74 (2006) 245109.
[24] R.J. Gambino, T.R. Mcguire, Y. Nakamura, J. Appl. Phys. 38 (1967) 1253–1255.
[25] G. Kresse, J. Hafner, Phys. Rev. B 47 (1993) 558;
G. Kresse, J. Hafner, Phys. Rev. B 49 (1994) 14251.
[26] G. Kresse, J. Furthmüller, Comput. Mater. Sci. 6 (1996) 15.
[27] G. Kresse, J. Furthmüller, Phys. Rev. B 54 (1996) 11169.
[28] G. Kresse, D. Joubert, Phys. Rev. B 59 (1999) 1758.
[29] J.Z. Peng, Y.F. Wang, M.F. Gray, Physica B 403 (2008) 2344–2348.
[30] D.W. Zhou, P. Peng, J.S. Liu, J. Alloys Compd. 428 (2007) 320.
[31] M.M. Wu, L. Wen, B.Y. Tang, L.M. Peng, W.J. Ding, J. Alloys Compd. 506 (2010) 413.
[32] R. Skála, M. Drábek, Bull. Czech. Geol. Surv. 76 (2001) 209–216.
[33] S. Rundqvist, Z. Anorg. Allg. Chem. 627 (2001) 2257–2260.
[34] S. Rundqvist, Acta Chem. Scand. 16 (1962) 287–292.
[35] W. Jeitschko, U. Flörke, U.D. Scholz, J. Solid State Chem. 52 (1984) 320–326.
[36] W. Jeitschko, A.J. Foecker, D. Paschke, M.V. Dewalsky, C.B.H. Evers, B. Künnen, A. Lang, G. Kotzyba, U.C. Rodewald, M.H. Möller, Z. Anorg. Allg. Chem. 626 (2000) 1112–1120.
[37] G.C. Zhou, L.Z. Sun, X.L. Zhong, X.S. Chen, J.B. Wang, Allg. Chem. Phys. Lett. A 368 (2007) 112–116.
[38] W. Tang, E. Sanville, G. Henkelman, J. Phys.: Condens. Matter. 21 (2009) 084204.
[39] G. Henkelman, A. Arnaldsson, H. Jónsson, Comput. Mater. Sci. 36 (2006) 354–360.
[40] I.R. Shein, A.L. Ivanovskii, J. Nucl. Mater. 393 (2009) 195.